

# Microstructural evolution of nanocrystalline $\text{Al}_2\text{O}_3$ sintered at a high heating rate

Fancheng Meng<sup>a,\*</sup>, Zhengyi Fu<sup>b</sup>, Weimin Wang<sup>b</sup>, Qingjie Zhang<sup>b</sup>

<sup>a</sup> *Department of Materials, Chongqing University of Technology, Chongqing 400050, China*

<sup>b</sup> *State Key Lab of Advanced Technology for Materials Synthesis and Processing, Wuhan University of Technology, Wuhan 430070, China*

Received 25 May 2009; received in revised form 13 July 2009; accepted 10 September 2009

Available online 29 October 2009

## Abstract

Experimental sintering studies on  $\text{Al}_2\text{O}_3$  powder (200 nm and 600 nm) were done at a heating rate of 1600 °C/min. The microstructural changes of specimens were examined and corresponding detailed data on the densification and grain size as a function of sintering time were presented. The grain-growth transition behavior during sintering was discussed. The results showed that the neck growth caused principally by surface diffusion could be negligible within 2 min. With subsequent increases of sintering time, grain growth promoted by grain boundary and lattice diffusion occurred.

Crown Copyright © 2009 Published by Elsevier Ltd and Techna Group S.r.l. All rights reserved.

**Keywords:** Alumina; Fast sintering; Fine grain; Densification

## 1. Introduction

Recently, densification of nano-grained ceramics has generated considerable interest. Dense ceramics with a fine grain structure are desirable, because a smaller size results in enhanced mechanical, high temperature, and optical properties [1–3].

One of the primary goals in the processing of nano-grained ceramics is the production of full-dense bodies while retaining the grain size on the nanometer scale. However, to obtain full density while preserving their nanostructure character is still a challenging task. This is mainly due to the inevitable grain growth during the final stage of sintering. In addition, the relatively slow heating rates used in conventional sintering allow significant heating durations up to the sintering temperature, during which the nanoparticles may coarsen.

Nowadays, a new fast fabrication technique for nano-grained materials has been developed [4]. The heat generated by a combustion reaction or self-propagating high-temperature synthesis (SHS) was applied to act as a high-temperature source, which was also called an “SHS furnace”. A large

mechanical pressure was applied when the sintering temperature reached the maximum. Full-dense nano-grained alumina ceramics with almost no grain growth were obtained under a pressure of 120 MPa in 2 min. However, there was little knowledge about grain-growth kinetics as well as densification mechanism at such high heating rate. Clearly, our ability to understand and control the grain-growth behavior can be a key factor in the optimization of the densification process. Optimization of the process parameters is also essential for preserving the nanostructure character of the fully dense compacts. In this presentation we will focus on the grain-growth kinetics and densification process in order to understand this superfast densification mechanism well.

## 2. Experimental procedure

The experimental procedure for the fabrication of nano-grained alumina specimen was described in our previous study in detail [4]; it is mentioned only briefly here.

Two kinds of  $\alpha\text{-Al}_2\text{O}_3$  powders (Sumitomo Chemical Co., Tokyo, Japan) with different particle sizes (200 nm and 600 nm) were used in this experiment. A fine powder (200 nm) was designated as F and a coarse powder (600 nm) was designated as C. The powders (F or C) were uniaxially pressed in a steel die into disks with a diameter of 2 cm and a

\* Corresponding author. Tel.: +86 23 62408527.

E-mail address: [mengfancheng@cqit.edu.cn](mailto:mengfancheng@cqit.edu.cn) (F. Meng).

height of 1 cm. Then, they were subjected to cold isostatic pressing (CIP) at 200 MPa.

An SHS reaction was chosen as follow:



The  $\text{Cr}_2\text{O}_3$ , Al, and C powders were mixed in a molar ratio of 3:6:4 according to the above reaction. In conventional sintering, the microstructure (grain size and density) is directly controlled by altering the sintering time under a certain temperature. In this novel sintering technique, the sintering times were conducted by varying the mass of SHS mixtures. In the combustion synthesis process, the combustion time can be altered by addition or decrease the mass of initial reactant powders. Owing to the same composition and particle size of the reactant mixture, the maximum reaction temperature and heating rate would remain near constant [5]. Series of sintered samples were prepared by using the different weight SHS powders. The weight of SHS powders was varied from 100 g to 1500 g with an interval of 100 g. With the variation of the SHS reactant mass, the sintering times were ranging from 1 min to 10 min. The different mass mixtures with CIP alumina body in the center were pressed into a cylindrical compact in different diameters and heights. The combustion processes was carried out in a homemade instrument and the details of the technique were given in Ref. [4]. The temperature of the alumina was measured using a WRe5/26-type thermocouple inserted in the center of the alumina. The measured maximum temperatures were maintained within  $1660 \pm 20^\circ\text{C}$  and had the same heating rate of  $1600^\circ\text{C}/\text{min}$ . In the conventional sintering, the holding times was easily controlled at a certain temperature. However, this is more difficult for SHS because of the high reaction rates. For a concise illustration, holding times were selected to the duration of the temperature higher than  $1550^\circ\text{C}$ . The density range and microstructure variation were adjustable at  $1550^\circ\text{C}$  using different sintering times.

The initial density of the green sample was calculated by measuring the dimensions of the sample. The sintered density was measured by Archimedes principle. The microstructures of the samples were investigated via field-emission scanning electron microscopy (FESEM, FEI-Sirion200, Amsterdam, the Netherlands). The grain size was measured from the SEM micrographs by the intercept method.

### 3. Results and discussion

#### 3.1. Grain-growth kinetic

The average grain size and relative density as a function of sintering time are displayed in Fig. 1. The relative density and grain size increased with increasing time. For powder C, when the holding time was 2 min, the relative density was about 82%. When the holding time increased from 3 min to 9 min, the relative density increased from 86% to 96%. For powder F, the relative density was slightly higher than that from powders C under the same sintering time. Fig. 1 also shows the change of

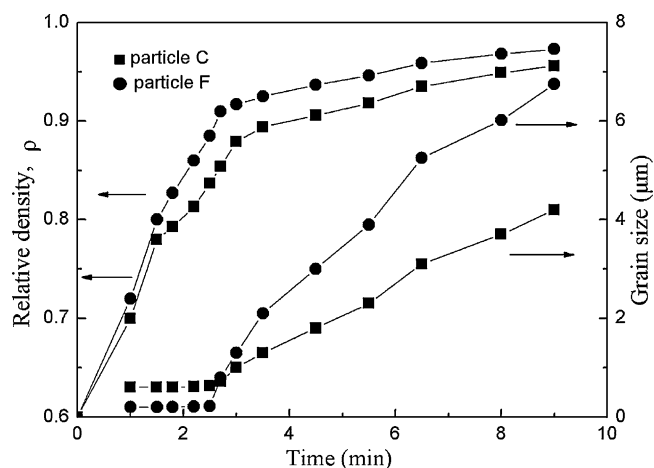


Fig. 1. Dependence of relative densities and grain sizes of sintered F and C on the sintering time.

grain size with different holding time. No obvious increase in size was seen as the holding time increased from 1 min to 3 min. With subsequent increase in sintering time, the grain size increased in an apparent linear fashion. At a holding time of 9 min, the sizes of powder C and F were increased to about  $4\ \mu\text{m}$  and  $7\ \mu\text{m}$ , respectively.

#### 3.2. Grain-growth developments

The microstructure developments of the sintered F and C at different holding times are illustrated in Figs. 2 and 3, respectively. The SEM images (Figs. 2(A) and 3(A)) showed that the specimens (holding time 2 min) consisted of grains of approximately the same size as the corresponding initial powders. Moreover, there were no obvious neck-growth and grain-shape change. Some pores between  $\text{Al}_2\text{O}_3$  grains were found and the pore structure consisted of open channels (open porosity) surrounded by three or more grains. As the sintering time increased, some grain-neck formed and grain-shape had an obvious change (Figs. 2(B) and 3(B)). The grains had an obvious growth and the sample appeared a chainlike structure (Fig. 2(B)). Some pore channels had collapsed and were found to be isolated (Fig. 3(B)). With the further increase of sintering time, the grain size of sample C and F increased greatly to  $4\ \mu\text{m}$  and  $7\ \mu\text{m}$  respectively (Figs. 2(C) and 3(C)).

#### 3.3. Grain-growth transitions

The result of the grain-size measurements (specimens F and C) is plotted vs. relative density in Fig. 4. The high-temperature holding time was varied from 1 min to 9 min. Within relative density regime I, no grain growth took place. Whereas in regime II densification occurred accompanied by very limited grain growth. Within higher density regime III fast grain growth occurred. It is obvious that the grain growth is quite fast with the increase of sintering time, implying that both grain-boundary migration and grain-boundary diffusion are enhanced.

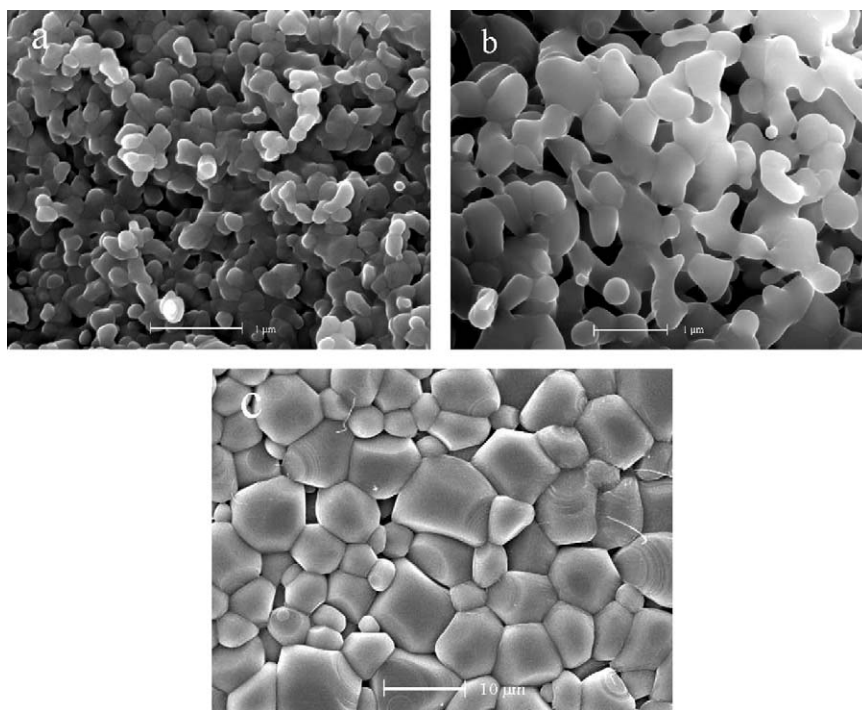


Fig. 2. SEM micrographs of fracture surfaces of sintered specimen F for different sintering time (a) 2 min; (b) 2.7 min; (c) 9 min.

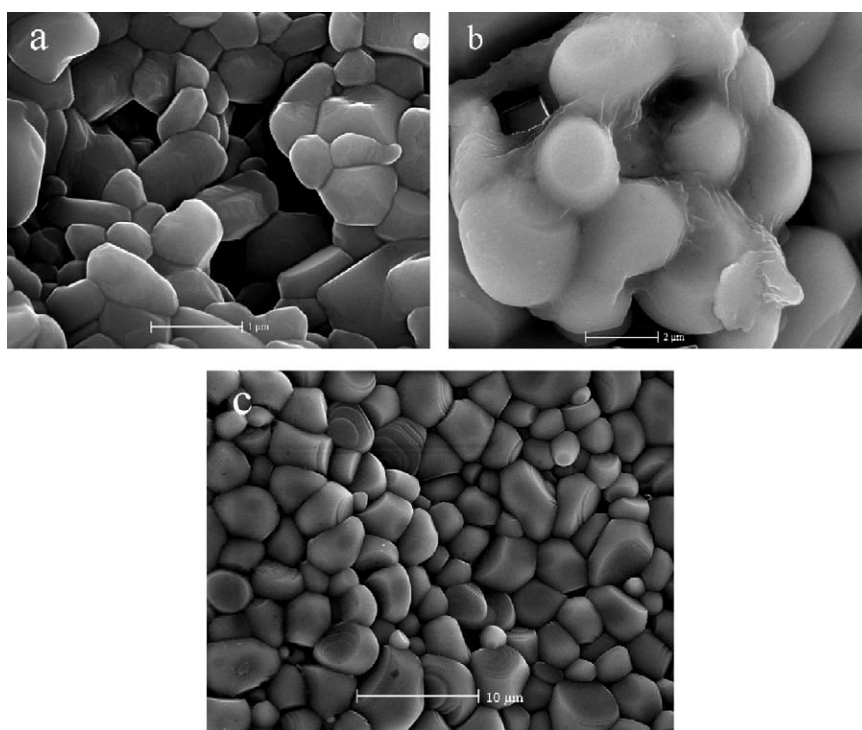


Fig. 3. SEM micrographs of fracture surfaces of sintered specimen C for different sintering time (a) 2 min; (b) 3.5 min; (c) 9 min.

From the relationship between the grain size and density, it was found that the grain-growth behavior fell into two distinct regions. In the region where the relative density was lower than 90%, grain growth was negligible; when the relative density grew over 90%, grains grew rapidly.

For comparison, calculations of grain-growth transition were also made using the relationship proposed by Raj et al.

The equation can be expressed in the general form [6–8]:

$$\ln \left[ \frac{1 - \rho}{1 - \rho_0} \right] = - \left( \frac{1}{\tau} \right) t \quad (2)$$

The transition in the grain-growth rate can be obtained by plotting  $[\ln(1 - \rho) - \ln(1 - \rho_0)]$  vs.  $t$ ; the value of  $\rho$  is the

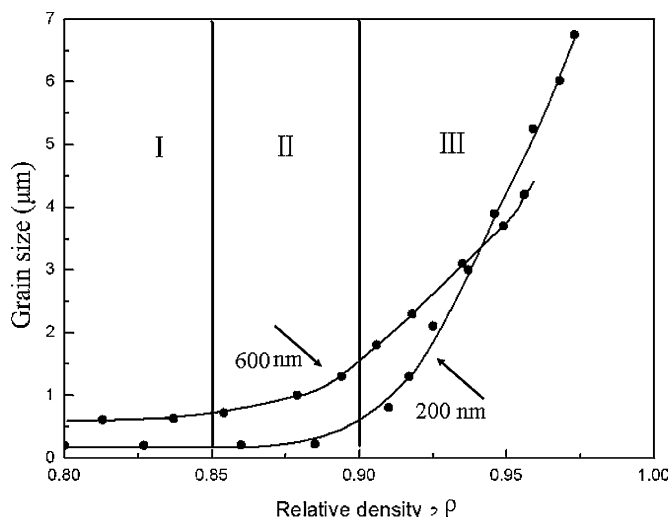


Fig. 4. Relative density vs. grain size curve of sintered specimen F and C.

instantaneous relative density,  $\rho_0$  is the green body density, and  $t$  is the sintering time.  $\tau$  is a time constant, which depends on the grain size,  $d$ , and the temperature [6–8]. In the case of a ceramic at certain temperature, the parameter  $\tau \propto d^3$ , and  $\tau$  will change with grain growth through the diffusion kinetics. Since  $\tau$  depends on the grain size, the slope will change if there is grain growth. If the grain size remains constant, then a linear fit to Eq. (2) is expected. If the grains begin to grow at a certain point, then that would be reflected in a change in the slope of the data when fitted to Eq. (2).

The plot of  $[\ln(1 - \rho) - \ln(1 - \rho_0)]$  vs.  $t$  is shown in Fig. 5. The sintering data between density and time were presented in Fig. 1. The calculated result indicated that the grain-growth transition occurred at relative density of near 90%. The region of  $\rho < 0.9$  showed a reasonably linear fit. Different time constant was found when the relative density was higher than 90%. The transition from a high time constant to a low time constant could be due to a fundamental change in the morphology of the sintering microstructure. This agrees with the experiment observation. Detailed microstructural analysis

has also provided a confirmation of this result. Similar behavior was observed on ZnO reported by De Jonghe et al. [9]. Wong and Pask [10] and Cameron and Raj [6] also showed that the time constants for intermediate-stage sintering and final-stage sintering were different using this formulation.

### 3.4. Discussions on grain-growth mechanism

In the preparation of nano-grained ceramics, surface diffusion is a dominating diffusion mechanism in the initial and intermediate stages of sintering, compared to grain boundary and lattice diffusion. This diffusion generally results in the grain-shape change and grain coarsening. The neck growth and further grain growth caused principally by surface diffusion mechanism have been proved in both experiment and theory calculation [11–13]. The calculations of Wilson showed that neck growth in the sintering of  $\text{Al}_2\text{O}_3$  must occur primarily by surface diffusion. The ratio of the neck-growth rate by surface diffusion to that by boundary diffusion in alumina with 10 nm particle size was also calculated to be as high as 105 [13]. It had been demonstrated that only surface diffusion contributed to neck growth during the initial sintering stage of  $\text{Al}_2\text{O}_3$  at 900 °C [14]. Surface diffusion on  $\text{TiO}_2$  particles was also observed directly for both grain growth and densification in the initial and intermediate sintering stages, which is accompanied by the diminishing of smaller grains [11]. That coarsening is considered to be detrimental to the preparation of nanoceramics.

Our results indicate that: the effect of fast heating rate and sintering times on grain growth appears obvious. The grain growth caused principally by surface diffusion has almost been avoided at a certain sintering condition. At a fast heating rate, the sample quickly skips over a low-temperature regime (nondensifying mechanisms such as surface diffusion active) and proceeds directly to higher temperatures. At the same time, densifying mechanisms (such as grain boundary or volume diffusion active) are in control within a short sintering time. Therefore, the grain growths beginning at the initial and intermediate stages of sintering can be controllable. The original nanostructure grain size may be preserved. This result was obtained in the intermediate stage of sintering, which is for  $0.80 \leq \rho \leq 0.90$ . With increasing sintering time, neck growth occurs. With further growth, the neck disappears by multiple transport mechanisms, e.g. surface, grain boundary, and volume diffusion. This period enters the final stage of sintering and the relative density is higher than 0.90. Thus, by using fast heating rate, significant control can be exerted over the mass transport mechanisms, microstructure evolution, and final microstructure.

### 4. Conclusion

Two kinds of  $\text{Al}_2\text{O}_3$  powders (200 nm and 600 nm) were sintered at 1550 °C with the heating rate of 1600 °C/min using SHS-furnace method. The microstructural changes and the densification, grain growth as a function of sintering time were discussed. The relative density and grain size of both specimens

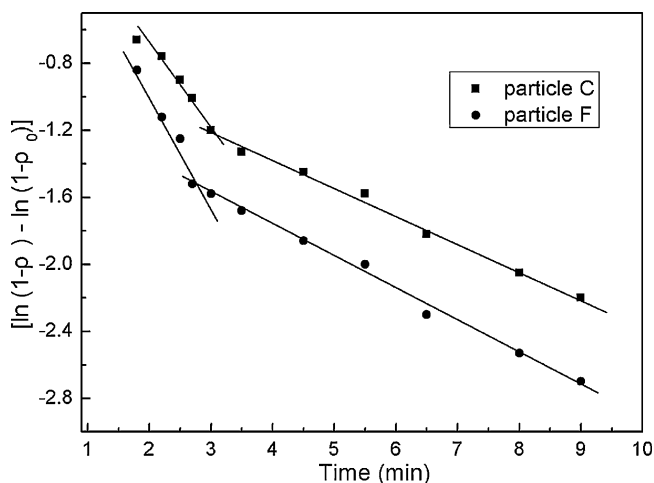


Fig. 5. The plot of  $[\ln(1 - \rho) - \ln(1 - \rho_0)]$  vs.  $t$  of sintered F and C.

increased with the increasing sintering time from 1 min to 9 min. The grain growth promoted by surface diffusion was limited within 2 min. Grain-growth transitions occur at relative densities of about 0.9. After that transition, the grain growth promoted by grain boundary and lattice diffusion was stronger and grains grew rapidly.

### Acknowledgements

This work has been financially supported by the Ministry of Education of China (PCSIRT0644), the National Natural Science Foundation of China (50772081, 50821140308) and Natural Science Foundation Project of CQ (CSTC 2009BB4385).

### References

- [1] A. Krell, P. Blank, Grain size dependence of hardness in dense submicrometer alumina, *J. Am. Ceram. Soc.* 78 (4) (1995) 1118–1120.
- [2] R. Riedel, H.J. Kleebe, H. Schnfelder, F. Aldinger, A covalent micro/nano-composite resistant to high-temperature oxidation, *Nature* 374 (1995) 526–528.
- [3] R. Apetz, M.P.B. van Bruggen, Transparent alumina: a light-scattering model, *J. Am. Ceram. Soc.* 86 (3) (2003) 480–486.
- [4] F.C. Meng, Z.Y. Fu, J.Y. Zhang, H. Wang, W.M. Wang, Y.C. Wang, Q.J. Zhang, Rapid densification of nano-grained alumina by high temperature and pressure with a very high heating rate, *J. Am. Ceram. Soc.* 90 (4) (2007) 1262–1264.
- [5] Z.Y. Fu, W.M. Wang, H. Wang, R.Z. Yuan, Z.A. Munir, Fabrication of cermets by SHS-QP method, *Int. J. SHS* 2 (3) (1993) 307–313.
- [6] C.P. Cameron, R. Raj, Grain-growth transition during sintering of colloidal prepared alumina powder compacts, *J. Am. Ceram. Soc.* 71 (12) (1988) 1031–1035.
- [7] R.K. Bordia, R. Raj, Analysis of sintering of a composite with a glass or ceramic matrix, *J. Am. Ceram. Soc.* 69 (3) (1986) C-55–C-57.
- [8] R.K. Bordia, R. Raj, Sintering of  $\text{TiO}_2\text{--Al}_2\text{O}_3$  composites: a model experimental investigation, *J. Am. Ceram. Soc.* 71 (4) (1988) 302–310.
- [9] L.C. De Jonghe, M.N. Rahaman, C.H. Hsueh, Transient stresses in bimodal powder compacts during sintering, *Acta Metall.* 34 (7) (1986) 1467–1471.
- [10] B. Wong, J.A. Pask, Models for kinetics of solid state sintering, *J. Am. Ceram. Soc.* 62 (3–4) (1979) 138–141.
- [11] J.L. Shi, Relation between grain growth, densification and surface diffusion in solid state sintering—a direct observation, *J. Mater. Sci.* 40 (2005) 5711–5719.
- [12] J.L. Shi, Relation between coarsening and densification in solid-state sintering of ceramics: experimental test on superfine zirconia powder compacts, *J. Mater. Res.* 14 (4) (1999) 1389–1397.
- [13] M.G. McKimpson, Densification maps for nano-sized powders, *Mater. Manuf. Process.* 11 (6) (1996) 935–949.
- [14] G. Greskovich, K.W. Lay, Grain growth in very porous  $\text{Al}_2\text{O}_3$  compacts, *J. Am. Ceram. Soc.* 55 (3) (1972) 142–146.